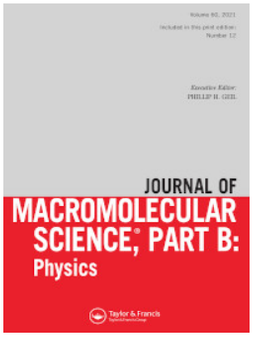

Taylor & Francis
Taylor & Francis Group

Journal of Macromolecular Science, Part B
Physics

ISSN: (Print) (Online) Journal homepage: https://www.tandfonline.com/loi/lmsb20

Relationship between the Deformation Processes Occurring in Rubbers and Their Molecular Structure

(Structure of Rubbers under Strain)

Vladimir I. Kartsovnik

To cite this article: Vladimir I. Kartsovnik (2021): Relationship between the Deformation Processes Occurring in Rubbers and Their Molecular Structure, Journal of Macromolecular Science, Part B, DOI: 10.1080/00222348.2021.2005914

To link to this article: https://doi.org/10.1080/00222348.2021.2005914

Published online: 18 Nov 2021.

JOURNAL OF MACROMOLECULAR SCIENCE, PART B
https://doi.org/10.1080/00222348.2021.2005914

Relationship between the Deformation Processes Occurring in Rubbers and Their Molecular Structure *(Structure of Rubbers under Strain)*

Vladimir I. Kartsovnik

The Society of Sciences & Engineering "KIW-Gesellschaft e. V.", Dresden, Germany

ABSTRACT

Based on measurements of rubber hysteresis curves, the relationship between the network structure of elastomers and their mechanical behavior is analyzed. On the basis of the classical theory of rubber elasticity, the Flory corrections, which take into account physical cross-links in the elastomer network structures in the course of straining a rubber sample at a constant rate, were calculated. To this end, the Frenkel-Eyring thermal-fluctuation theory was used, also taking into account the activation energy of the polymer viscosity, which depends on the entropic elasticity of macromolecules in the processes of their flow and deformation. Flory corrections were calculated within the standard linear solid model.

ARTICLE HISTORY
Received 6 March 2021
Accepted 7 November 2021

KEYWORDS
entropic elasticity of macromolecules; Eyring's viscosity theory; Flory's corrections factor; hysteresis curves; physical cross-links of elastomers networks; relation between the elastomer structure and their deformation properties

Introduction and experimental

The ability of elastomers to sustain high reversible deformations is associated with the entropic nature of the stretching behavior of long macromolecules in a condensed amorphous state. The statistical rubber elasticity theory, elaborated in its application to elastomer networks,[1] sets out the dependence between the true stress,σ_i, sustained by the elastomer, and the extended length of the specimen, l, in the following form[2]:

$$\sigma_i = nRT\left[(\frac{l}{l_0})^2 - \frac{l_0}{l}\right] = nRT\left(\lambda^2 - \frac{1}{\lambda}\right) \quad (1)$$

where λ is the extension ratio: $\lambda = \frac{l}{l_0} = \frac{l_0+\Delta l}{l_0} = 1 + \varepsilon$, l is the current length of the specimen, l_0 is the initial length in the specimen before the extension, $\Delta l = l - l_0$ is the difference between the specimen's current and initial length values, $\varepsilon = \frac{\Delta l}{l_0}$ is the relative elongation, $n = \frac{\rho}{M_c}$ is the number of moles of network chains found in a unit volume (cm^3), ρ is the elastomer density, M_c is the molecular weight of the chain segments between cross-links, R is the gas constant and T is the absolute temperature.

The isothermal Young's modulus,E, for any point of the strain curve, also called the rubbery modulus, can be expressed as the derivative of the force, σ_i, with respect to the strain, λ, at a given temperature[2]:

CONTACT Vladimir I. Kartsovnik vkartsovnik@googlemail.com The Society of Sciences & Engineering "KIW-Gesellschaft e. V.", Mohnstr. 22, 01127, Dresden, Germany.

$$E = \left(\frac{d\sigma_i}{d\lambda}\right)_T \tag{2}$$

After differentiating Eq. (1), we obtain Eq. (3), which gives the rubbery modulus, E, for the true stress σ_i :

$$E = nRT\left[2(\frac{l}{l_0})^2 + \frac{l_0}{l}\right] = nRT\left(2\lambda^2 + \frac{1}{\lambda}\right) \tag{3}$$

The magnitude of the length of the molecular chains M_c between the cross-links of rubber was taken into account by Flory[3] in Eq. (3) for the modulus of elasticity,E, of the network[1]:

$$E = g\frac{\rho RT}{M_c}\left(1 - \frac{2M_c}{M}\right) \tag{4}$$

where M_c is the molecular weight of a chain segment extending between inter-chain cross-links and M is the initial molecular weight of the elastomer before cross-linking, ρ is the density of the rubber. The values M_c and M were introduced by Flory to characterize the number of chemical cross-links in the network. To account for other potential defects of the network that may change the number of cross-links in the network and affect its deformation behavior, Flory introduced the correction factor g.

Using Flory's corrections g in Eq. (4) to account for network flaws, we obtain for Eq. (3) the following expression for the rubbery modulus:

$$E = g\frac{\rho RT}{M_c}\left(1 - \frac{2M_c}{M}\right)\left(2\lambda^2 + \frac{1}{\lambda}\right) \tag{5}$$

Flory's factor g can be calculated based on an analysis of tensile curves by measuring the isothermal Young's modulus,E (Eq. (5)) for any point of the strain curve.

Formula (1), however, was found to only be in agreement with the uniaxial extension curves obtained by experimentation when the extension ratios were small to medium.[1] In response to this issue, other dependences were developed to provide a more complete description of the tensile curves for rubber; these contained two, three or more parameters and had an empirical nature (Mooney-Rivlin's formula, Martin-Roth-Stiehler's formula, etc.).[4]

The statistical rubber elasticity theory (Eq. (1)) provides a good and multi-faceted description of elastomer deformation mechanisms. However, the fact that the theoretical dependence fails to match those shown by experimental tensile curves at high elongation calls for an explanation since it suggests that our understanding of how the structure of network elastomers relates to the mechanism governing their deformation may be incomplete. To elucidate such relationships we conducted our study of the mechanical hysteresis of rubber.

Changes in the structure during the stretching of rubbers are vividly manifested in the Mullins effect.[5] This effect is easily observed in the mechanical hysteresis curves for rubber. After a rubber specimen is extended for the first time and then allowed to recover from the deformation, repeated extension by the same amount requires significantly lower stress values. The hysteresis curves for a silicone rubber [poly(methylvinylsiloxane)] are shown in Fig. 1. We subjected the rubber specimen to tensile deformation

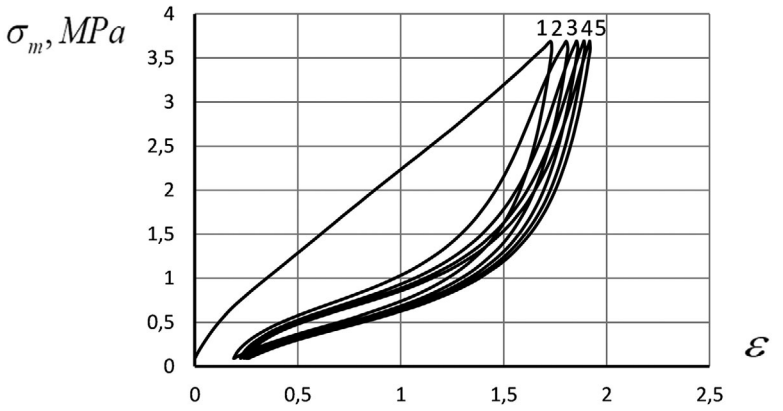

Figure 1. Hysteresis loops obtained for silicone rubber subjected to repeated forced extension, and compression at 250 mm/min at room temperature.

at 250 mm/min until the stress reading reached a specified nominal stress value of 3.8 MPa, calculated for the initial cross-section. After this, the specimen was subjected to reverse deformation until the stress had been completely relaxed. This was then repeated four times.

A strong shift of the first ascending tensile curve toward larger strain values for the repeat hysteresis loops indicated a significant softening of the material, which seems naturally attributable to a change in the elastomer structure. For unfilled rubber (here an elastic silicone rubber), such a structural change is most likely due to rupture of cross-links during the first round of deformation. What calls for additional research, however, are the ways in which we could refine our understanding of what type of cross-links (chemical or physical) have actually broken, and how the primary and, to a lesser extent, successive structural elements will change as the specimen is taken through further rounds of deformation.

Although the Mullins effect has been studied for over six decades, it is still considered a major challenge in explaining the behavior of rubber-like materials, not just in terms of understanding the underlying physics of this effect, but in terms of modeling it mechanically.

The purpose of our research described here was to analyze the hysteresis curves based on the basic provisions of the statistical theory of rubber elasticity, including some defects of the structure of elastomeric networks. The main mechanical property role of the various types of cross-links, providing highly elastic reversible deformation of the elastomer networks, is played by chemical cross-links. Flory drew attention to the entanglements of the chains as a flaw of the network.[3] These can have an effect similar to that of chemical cross-linking, although weaker.

Discussion

It seems only logical that the increase in tensile stress occurring in an elastomer undergoing tensile deformation at a constant rate,$\dot{\varepsilon}$, should be described in terms of the Standard Linear Solid (SLS) model. According to this model, an increase in applied

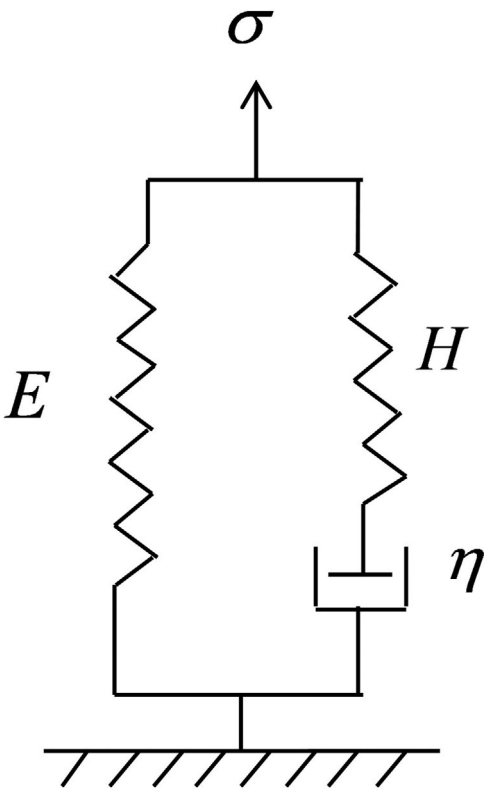

Figure 2. Standard Linear Solid (SLS) mechanical model.

stress,σ, increases the reversible strain governed by the modulus of the rubbery spring, E (Fig. 2):

For the SLS model, the external stress,σ, being applied is equal to the sum of the stresses on the rubber-like spring with modulus E and the elastic spring with modulus H. This can be written as $\sigma = \sigma_{en} + \sigma_e$. Here, $\sigma_{en} = f_{en}$ is the stress associated with the forces of entropic elasticity and reversible deformation, ε, generated by the elastomer, and σ_e is the stress on the elastic spring with modulus H; this stress, σ_e, is equal to the stress on the dashpot, σ_η, the viscous element of the SLS model. Provided that, for purposes of the SLS model, $\sigma_{en} = E\varepsilon_{en} = E\varepsilon$, the following expression for the stress, σ_η, on the dashpot is obtained:

$$\sigma_\eta = \sigma_e = \sigma - \sigma_{en} = \sigma - E\varepsilon \tag{6}$$

The differential equation for the SLS model is[6]:

$$\eta(H + E)\dot{\varepsilon} + HE\varepsilon = \eta\dot{\sigma} + H\sigma \tag{7}$$

In Eq. (7), η is the viscosity of the dashpot in the SLS model, H is the Hookés modulus of an elastic spring connected in series with the dashpot, E is the elastic modulus of the reversible (rubber-like) spring, ε is the relative strain, $\dot{\varepsilon}$ is the strain rate of deformation during stretching of the sample, and $\dot{\sigma}$ is the rate of change of stress when stretching rubber at a constant rate.

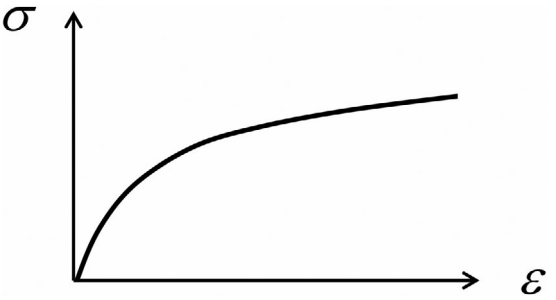

Figure 3. Stress-strain dependence for the SLS model with constant strain rate $\dot{\varepsilon}$.

For constant-viscosity η situations the SLS model predicts that, as the solid is extended at a constant rate, the strain-dependent stress growth will gradually slow down and evolve into a linear stress-strain dependence[6] (Fig. 3).

To express the stress-strain relation for rubber at constant tensile strain rate, $\dot{\varepsilon}$, we rewrite Eq. (7) as follows:

$$\eta(H+E)\dot{\varepsilon} - \eta\dot{\sigma} = H\sigma - HE\varepsilon \tag{8}$$

From this it can be written:

$$\sigma = \frac{\eta[(H+E)\dot{\varepsilon} - \dot{\sigma}] + HE\varepsilon}{H} = \eta\frac{(H+E)\dot{\varepsilon} - \dot{\sigma}}{H} + E\varepsilon \tag{9}$$

For the SLS model at a constant rate of deformation growth $\dot{\varepsilon} = const$ and the dashpot viscosity $\eta = Ae^{\frac{E_0}{k_B T}} = const$ (Arrhenius-Andrade equation) is independent of the applied load σ. Here E_0 is the activation energy of the flow in the Arrhenius-Andrade equation.[7] At the moment the external force σ is applied, the plunger resistance in the dashpot is at its maximum. This resistance decreases until the velocity of the plunger motion becomes equal to the strain rate $\dot{\varepsilon} = const$. Therefore, the stress growth rate $\dot{\sigma}$ in the graph of Fig. 3 for the SLS model decreases until the stress becomes proportional to the strain.

In contrast to the graph in Fig. 3, the experimental curves obtained for the actual behavior of rubbers under repeated stretching (Fig. 1) have a peculiar S-shaped form. At first, the stress growth slows down, to about 20%–30% of the deformation. After that, there is a rapidly accelerating growth in stress with an increase in deformation in the range from about 70% to 170%, as can be seen for curves 2–5 in Fig. 1. This dependence of stress σ on strain ε is close to an exponential dependence. It can be related to the exponential term $\eta = A\exp\frac{E_0}{k_B T}$ in Eq. (9). But this is the case if the viscosity η in the dashpot of the SLS model depends on the stress σ or strain ε.

The dependence of viscosity on stress for the flow of non-Newtonian liquids according to Eyring's equation is well known[7]:

$$\eta = Af\exp\frac{E_0 - bf}{k_B T} \tag{10}$$

Here A is the pre-exponential multiplier in the Eyring's equation calculated by absolute reaction rate theory, f is the shear stress at flow, b is the "viscous volume" coefficient by Eyring's, E_0 is the activation energy at 0°K, i.e. the height of the potential

energy barrier for jumping into a vacancy of the molecular-kinetic units (MKUs) during thermal motion of the molecules in the absence of external force, k_B is the Boltzmann constant, and T is the absolute temperature.

According to the statistical rubber elasticity theory,[1] the uncoiling of a macromolecular chain in a polymer under tension causes the forces of entropic elasticity that counteracts this tension, f_{en}, to increase in proportion to the distance, r, between the ends of the macromolecule:

$$f_{en} = \frac{3k_BT}{Nl^2}r \tag{11}$$

Here, N is the number of statistical units per chain and l is the length of each unit.

In a thermally-activated process governed by the Frenkel mechanism, the flow of free atoms or small molecules in a liquid proceeds by their jumping into vacancies as a result of their own thermal motion.[8] According to Eyring's equation (10), an external force, f, applied to such a system decreases the activation energy of the jump of atoms to the vacancy in the direction of the respective force.[7] Incidentally, a similar process of plastic deformation can also occur in metals when the effects of external forces on atoms are channeled through elastic interatomic linkages.[9]

As was shown in reference,[10] during the flow of polymeric fluids, the emerging forces of entropy elasticity, f_{en}, reduce the activation energy of the MKU jump in the direction of the external forces by a magnitude proportional to the entropic elasticity force.

In polymer networks, however, the entropic elasticity forces cause the opposite effect: they do not decrease, but increase the activation energy E_0 of MKU jumping into vacancies for the molecular chains of the elastomeric network.[11] The chains are stretched during the jumps of the MKUs into vacancies in the direction of the external force σ. As the chain is stretched, the entropic elasticity force, f_{en}, increases, and at a constant rate of stretching,$\dot{\varepsilon}$, the stress, σ, on the sample increases to overcome the potential barrier of the MKU jumping into vacancies in the stretching direction.

The process of deformation of the elastomeric chain in accordance with the SLS model proceeds as a viscoplastic flow with the unfolding of the polymer chains of the network in the direction of the external force, σ. The flow process is reflected in the SLS model as a dashpot with viscosity, η, and stress, σ_η, with the help of which the MKU jumps into the vacancy in the direction of sample deformation ε. Since, with increasing deformation, the chains are stretched and the force of entropic elasticity increases the resistance of the chains to an external force, σ, this means an increase in the potential energy barrier, E_0, for the MKU to jump into the vacancy in the direction of the deformation growth. In accordance with Eyring's derivation of formula,[7] for the flow processes in his Eq. (10), the activation energy should increase by an increase in the stress of the dashpot, σ_η.

In the case of elastomer extension, Eyring's formula for viscosity,η, would look like this:

$$\eta = A\sigma_\eta \exp\frac{E_0 + b\sigma_\eta}{k_BT} \tag{12}$$

Now the equation of viscosity, η, when stretching elastomers according to the SLS model, taking into account Eqs. (6) and (12), can be written as:

$$\eta = A(\sigma - E\varepsilon)\exp\frac{E_0 + b(\sigma - E\varepsilon)}{k_B T} \tag{13}$$

It follows that, under the SLS model, an increase in elastomer viscosity, η, upon deformation reflects an increase in the resistance of the macromolecules of the polymer network to the tensile stress generated when the elastomer is being extended.[11]

For the reverse deformation curves of a hysteresis loop, the entropic elastic forces, f_{en}, coincide with the retraction direction of the sample. The entropic elastic forces,f_{en}, because of the coiling chains, help jumping MKUs into vacancies during the retraction of the sample in the direction of decreasing deformation; i.e. the potential barrier, E_0, to moving the MKUs is decrease. For the SLS model, in this case, the viscosity, η, decreases by analogy with Eq. (10) and in accordance with Eq. (6): $\sigma_\eta = \sigma - E\varepsilon$.

$$\eta = A(\sigma - E\varepsilon)\exp\frac{E_0 - b(\sigma - E\varepsilon)}{k_B T} \tag{14}$$

The relationship between external forces,σ, and entropic elasticity forces, f_{en}, in the processes of stretching and retraction elastomeric networks allows us to estimate the exponential dependence of external stress, σ, on deformation, ε. To do this, we write Eq. (9) in the following form:

$$\sigma = \frac{(H+E)\dot{\varepsilon} - \dot{\sigma}}{H}\cdot A(\sigma - E\varepsilon)\exp\frac{E_0 \pm b(\sigma - E\varepsilon)}{k_B T} \pm E\varepsilon \tag{15}$$

The exponential term in Eq. (15) with a plus sign before the multiplier, $b(\sigma - E\varepsilon)$, contributes to the rapidly accelerating rate of stress increase as a function of the stress σ on the strain ε of the network when the sample is stretched, and with a minus sign before the multiplier, $b(\sigma - E\varepsilon)$, in the exponential dependence of the stress σ reduction on the deformation ε, during the retraction of the sample, i.e. during the decrease in the deformation when compressing for hysteresis loops.

Hysteresis measurements make it possible, therefore, to test the aforesaid influence of the forces of entropic elasticity, f_{en}, on the description of the strain curves for elastomers based on the differential equation of the SLS model (Eq. (7)). As a suitable tool, we can use Eyring's formula (Eq. (10)) modified for the tensile and reverse-tensile deformation scenarios, as shown in Eqs. (13) and (14).

Consider the possibility of confirming these deformation processes of elastomeric networks based on the example of the SLS model. We can now isolate the viscosity factor, η, from Eq. (7), rewritten as Eq. (16):

$$\eta(H+E)\dot{\varepsilon} - \eta\dot{\sigma} = H\sigma - HE\varepsilon \tag{16}$$

Hence,

$$\eta = \frac{H(\sigma - E\varepsilon)}{(H+E)\dot{\varepsilon} - \dot{\sigma}} \tag{17}$$

From Eqs. (13) and (17) we obtain:

$$\frac{H(\sigma - E\varepsilon)}{(H+E)\dot{\varepsilon} - \dot{\sigma}} = A(\sigma - E\varepsilon)\exp\frac{E_0 + b(\sigma - E\varepsilon)}{k_B T} \tag{18}$$

We write $\frac{A}{H} = C$, and after dividing both sides of Eq. (18) by the factor $H(\sigma - E\varepsilon)$, we obtain:

$$\frac{1}{(H+E)\dot{\varepsilon} - \dot{\sigma}} = C\exp\frac{E_0 + b(\sigma - E\varepsilon)}{k_B T} \tag{19}$$

Taking the logarithm of Eq. (19), we obtain Eq. (20):

$$\ln\frac{1}{(H+E)\dot{\varepsilon} - \dot{\sigma}} = \left(\ln C + \frac{E_0}{k_B T}\right) + \frac{b}{k_B T}(\sigma - E\varepsilon) \tag{20}$$

Based on the hysteresis curves constructed from the experimental data of specimens subjected to tensile loading, the rapidly accelerating ascending stretch curve should, under the SLS model, demonstrate a linear dependence of the value of $\ln\frac{1}{(H+E)\dot{\varepsilon} - \dot{\sigma}}$ on the value of $(\sigma - E\varepsilon)$ according to Eq. (20). In addition the value of the rubbery modulus, E, obtained from formula (5), should also change as the extension ratio, $\lambda = 1 + \varepsilon$, increases.

A similar linear dependence (20), but with a reverse sign, with a magnitude $\frac{b}{k_B T}(\sigma - E\varepsilon)$, must be observed during retraction of the rubber sample for the reverse deformation of the hysteresis loop in accordance with the scheme shown in Fig. 5.

$$\ln\frac{1}{(H-E)\dot{\varepsilon} - \dot{\sigma}} = \left(\ln C + \frac{E_0}{k_B T}\right) - \frac{b}{k_B T}(\sigma - E\varepsilon) \tag{21}$$

The linearization of the experimental hysteresis curves in accordance with Eqs. (20) and (21) will confirm the correctness of the proposed schemes of the effect of entropic elasticity forces, f_{en}, on the processes of stretching and retraction of elastomeric networks.

Experimental results

Rubber hysteresis was measured using a Zwick-Z 010 testing machine (the ZwickRoell Group, ZwickRoell GmbH & Co., KG, Germany) complete with a MultiXtens extensometer in accordance with DIN EN ISO 527-2/S2. The tests used dumbbell shaped specimens of rubber according to ISO 527-2 in the form of a flat strip with a rectangular narrow section of length 43 mm. The rectangular sections were 2 mm thick and 4 mm wide. The test length of a specimen, as measured with an extensometer, was 15 mm. Series of hysteresis curve measurements were performed at extension rates of 250 and 25 mm/min at room temperature (each series was repeated on a new specimen to assess the reproducibility of the results). More tests were then performed at 50 °C (2 series for reproducibility), 75 °C (3 series) and 100 °C (2 series), all at an extension rate of 25 mm/min.

In each series the rubber specimens ware each taken through 5 rounds of tensile deformation. The deformation was terminated when the stress reading reached the specified nominal value of *ca.* 3.8 MPa. Each deformation round was immediately followed by reverse deformation at a retraction rate equal to the extension rate used earlier

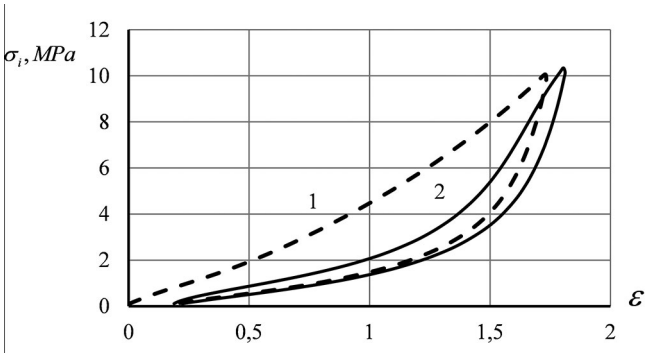

Figure 4. True stress vs. strain dependence for silicone rubber at room temperature with an extension rate of 250 mm/min for the first (dashed line 1) and second (solid line 2) hysteresis cycles from Fig. 1.

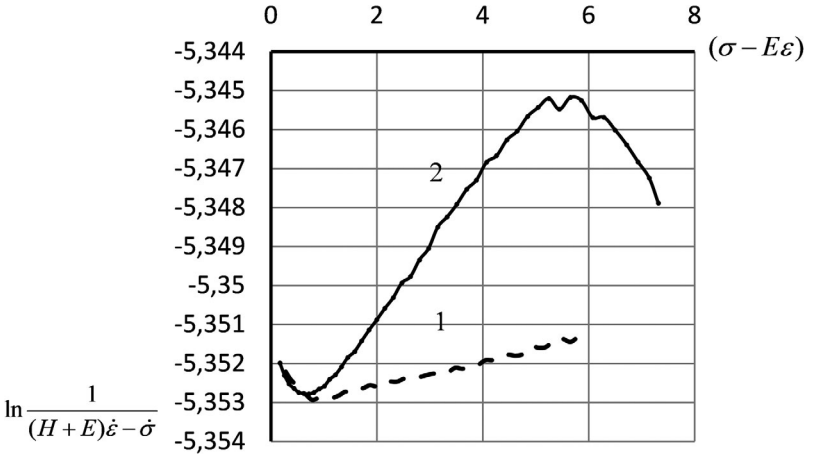

Figure 5. Dependence of $\ln\frac{1}{(H+E)\dot{\varepsilon}-\dot{\sigma}}$ on $(\sigma - E\varepsilon)$ for the ascending strain curve legs describing the first hysteresis cycle from Fig. 4 (dashed line 1) and the second hysteresis cycle from Fig. 4 (solid line 2).

until the stress reading returned to the initial value of 0.1 MPa, whereupon the specimen was immediately stretched again (Figs. 1 and 4).

The material used for the experiment was a silicone rubber based on poly(methylvinylsiloxane) (PMVS), as we used in Ref. [12]. The molecular weight inputs used in formula (5) to calculate the rubbery modulus, E, were the molecular weight of a chain segment extending between chemical cross-links, taken as $M_c = 80,000$, and the average molecular weight for the PMVS, taken as $M = 600,000$. With these inputs, the formula used to calculate the rubbery modulus E, based on Eq. (5) above, was Eq. (22):

$$E = g \cdot 0,0227 \cdot \left(2\lambda^2 + \frac{1}{\lambda}\right) \tag{22}$$

Figure 4 compares the first (dashed line) and second (solid line) hysteresis curves, shown in Fig. 1, but plotted in the true stress vs. strain coordinates. Experimental data for the ascending tensile strain curves describing the first (1) and second (2) hysteresis

Table 1. Flory's corrections for linear segments according to dependencies (20) and (21) for the increasing deformation of the hysteresis cycles from Figs. 4 and 5.

Hysteresis cycle number	Strain ascension interval	g	R^2	$\frac{b}{k_B T}$
1	1.8%–20.0%	24	0.9956	−0.0037
1	21%–170%	0.6	0.9960	+0.0003
2	21%–56%	10	0.9907	−0.004
2	65%–164%	4.5	0.9975	+0.0019
2	166%–179%	0.1	0.9512	−0.0012

cycles were calculated using Eqs. (20) and (21), with the results shown in the graph in Fig. 5.

The linear dependence expressed in Eq. (20) or (21) for the initial, decelerating segment (from $\varepsilon = 0.018$ to $\varepsilon = 0.2$ Fig. 4, Table 1) and the main ascending segment (from $\varepsilon = 0.2$ to $\varepsilon = 1.7$, Fig. 4) of the hysteresis curves makes it possible to determine the values of Flory's correction, g, in Eqs. (5) and (22). This can be achieved by selecting the value of the rubbery modulus, E, according to Eq. (22), when analyzing the experimental data for the graph in Fig. 5, such that the best possible linearity is achieved for the linear dependences (20) and (21) for all cycles, as suggested in [12]. The Hooke modulus, H, in the SLS model and in Eqs. (20) and (21), can be calculated as the limiting modulus for the glassy state in terms of the solubility parameter for a particular polymer.[2] For silicone rubber,g, according Table II,3 Tobolsky's,[2] the value of the solubility parameter was $\delta = 7.3(\mathrm{cal/cm^3})^{1/2}$. From this one can calculate the value $H = 1793\,\mathrm{MPa}$. Flory's correction factor, g, calculated for the maximum correlation coefficient of the linear regression of Eqs. (20) and (21), can be used to indicate the number of labile physical cross-linkages which can participate in the deformation process when a given elastomer network is being extended at a given rate $\dot{\varepsilon}$ in a given temperature environment specified for rubber tensile tests.

The two sections in the graph in Fig. 5 for the increasing tension curve of the first hysteresis loop (dashed lines) correspond to the two characteristic segments of the rubber tension curve in Fig. 4. In the initial small segment of this tensile curve, in the strain interval from $\varepsilon = 0.02$ to $\varepsilon = 0.20$ $[(\sigma - E\varepsilon) = 0.169$ to $0.714]$, a decrease in the rate of stress growth with increasing strain was observed. The second, basic segment of the tensile curve, in the interval from $\varepsilon = 0.2$ to $\varepsilon = 1.7$ $(\sigma - E\varepsilon) = 0.778$ to $5.804)$, shows a rapidly accelerating stress increase with increasing strain.

A possible explanation is as follows. At small deformations, the displacement of molecular-kinetic units of polymer chains with accompanying destruction of weak intermolecular bonds between them occurs. Their movement corresponds to the plastic flow of the material. Moving free chain ends can also be described as a flow process. Plastic flow is accompanied by a decrease in the activation energy in the Eyring's equations (10) and (14) for the SLS model[10] with the minus sign before the viscous element stress, $\sigma_\eta = \sigma - E\varepsilon$. A decrease in the number of intermolecular bonds that hold the chains reduces the viscosity, η, of the medium.

As the tensile process continues, the material's response to it begins to change when the stretching of the polymer chains comprising the main elastomer network comes strongly into play. The resistance of these chains to external loading increases the activation energy due to the growth of the entropic elasticity forces, f_{en}, of the macromolecules in accordance with relation (12), (13), and (20).

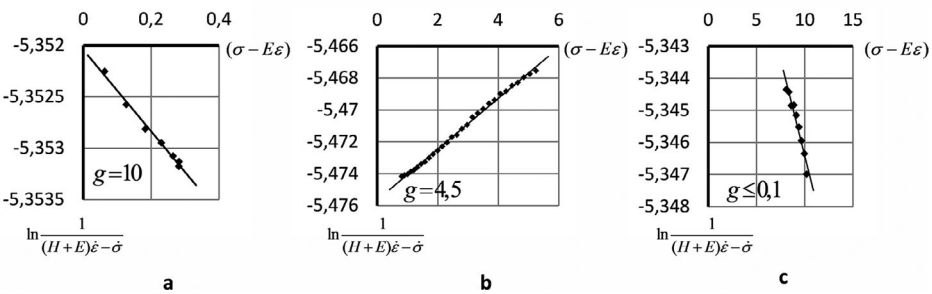

Figure 6. Approximation of Eqs. (20) and (21) for the initial (a), main (b) and final (c) linear segments of the ascending strain curve leg describing the second hysteresis cycle in Fig. 4.

Table 2. Flory's correction factors for the main and final segments of the reverse strain curve legs describing the hysteresis cycles from Figs. 4 and 5.

Hysteresis cycle number	Strain reversal interval	g	R^2	$\frac{b}{k_BT}$
1	173%–103%	7	0.9985	−0.0042
1	65%–25%	70	0.9993	+0.0005
2	178%–81%	5.65	0.9971	−0.0038
2	70%–29%	81	0.9984	0.0005

Consideration of the results

The details of the strain curves for the first and subsequent repeat hysteresis cycles reflect the connection between the deformation processes occurring in rubbers and related changes in their molecular and supramolecular structure. Let us consider, step-by-step, possible explanations for these connections, working on the premise that the dependences in Eqs. (12), (13), and (19)–(21) hold.

1. For all series of hysteresis cycles, the ascending leg of the first-cycle strain curve usually has two segments where the linear dependences per Eqs. (20) and (21) visibly hold.
2. Another important fact concerning namely the repeated curves of the hysteresis cycle is that they began to have a third segment in the ascending tensile curve leg during the subsequent stress applications corresponding to the final stages of the tensile deformation process. Namely, the deceleration of the stress growth of the tension curve in the strain interval of 1.66–1.79 (solid line in Fig. 4). When the curve data were analytically transformed to fit the coordinates of Eqs. (20) and (21), this growth deceleration becomes manifest in the term $(b/k_BT)(\sigma - E\varepsilon)$ (Table 1), which took on a negative value, as can be seen in the graph in Figs. 6(a) and 6(c) (below).

   In other words, there is a decrease of resistance of entropic elasticity forces to external stress σ. The most plausible explanation for this fact is the breaking of chemical bonds and their accompanying physical bonds ($g \approx 0.1 - 1.3$, see Tables 3–7) in parts of the network when stretching the constituent chains beyond their ultimate tensile strength; the viscosity of the medium decreases due to a reduction in the number of network chains that resist the external force.

Table 3. Flory's corrections for linear segments of dependences (20) and (21) for hysteresis curves with an extension rate of 250 mm/min at room temperature.

Hysteresis loop number Strain Curve Segment Number	1	2	3	4	5
1, deformation, %	1.8–20	21–56	24–53	26–57	27–49
Flory's correction factor, g	24	10	9	8.8	9
2, deformation, %	20–167	65–164	82–176	87–182	68–185
Flory's correction factor, g	0.6	4.5	4	4.5	5
3, deformation, %	–	166–179	177–185	184–188	188–190
Flory's correction factor, g	–	0.1	0.1	1.3	0.3
4, deformation, %	172–103	178–81	184–105	189–71	191–76
Flory's correction factor, g	7	5.65	5.8	5.6	5.5
5, deformation, %	65–25	70–29	73–31	71–30	76–26
Flory's correction factor, g	70	81	127	150	95

Table 4. Flory's corrections for linear segments of dependences according to Eqs. (20) and (21) for hysteresis curves obtained at an extension rate of 25 mm/min at room temperature.

Hysteresis Loop number Strain Curve segment number	1	2	3	4	5
1= ascending, initial	23	10	9	8.5	8.3
2= ascending, main	0.1	5	5	5	5
3= ascending, final	–	0.2	0.1	0.1	0.2
4= reverse, main	6.5	5.5	6	5.9	6
5= reverse, final	139	72	71	51	93

Table 5. Flory's corrections for linear segments of dependences according to Eqs. (20) and (21) for hysteresis curves obtained at an extension rate of 25 mm/min at 50 °C.

Hysteresis Loop number Strain Curve segment number	1	2	3	4	5
1= ascending, initial	21	10	9.5	10	9
2= ascending, main	0.4	5	5	5	5
3= ascending, final	–	0.2	0.2	0.8	0.5
4= reverse, main	6	6	6	6	5
5= reverse, final	32	43	34	42	51

Table 6. Flory's corrections for linear segments of dependences according to Eqs. (20) and (21) for hysteresis curves obtained at an extension rate of 25 mm/min at 75 °C.

Hysteresis Loop number Strain Curve segment number	1	2	3	4	5
1= ascending, initial	16	10.2	12	11	9
2= ascending, main	0.2	5.5	6	6	6
3= ascending, final	–	0.2	0.1	0.9	0.5
4= reverse, main	7	6.7	6.3	6	6
5= reverse, final	40	39	73	39	55

This is also reflected in Eq. (14) as a decrease of total activation energy $[E_0 - b(\sigma - E\varepsilon)]$ in the viscosity exponent. In addition, the torn network fragments represent the free ends of the chains. During further stretching, the entropic

Table 7. Flory's corrections for linear segments of dependences according to Eqs. (20) and (21) for hysteresis curves obtained at an extension rate of 25 mm/min at 100 °C.

Hysteresis Loop number Strain Curve segment number	1	2	3	4	5
1= ascending, initial	23	12	11	10.7	10.5
2= ascending, main	0.1	6	6	6.5	7
3= ascending, final	–	0.2	0.3	0.4	4.5
4= reverse, main	8	7	6.5	6.75	6
5= reverse, final	74	80	82	65	74

elastic forces cause these free ends to coiling in the direction of deformation. This is similar to the polymer chain flow process and is described as viscosity reduction[10] by Eqs. (10) and (14).

Flory's correction factors, g, were calculated using Eqs. (20) and (21) based on the best possible linearity solutions for the linear segments of the experimental curves in Fig. 5. The Flory corrections were calculated for the linear segments of increasing deformations of the first hysteresis cycle (dashed line) and the second hysteresis cycle (solid line) shown in Fig. 5. They are listed in Table 1. Table 1 also presents the correlation coefficients, R^2, for the linear dependences (20) and (21) and the slope values, $\frac{b}{k_B T}$, for these dependences, with the results described in Sec. 3 below.

3. Table 1 data for the first hysteresis loop shows that the beginning of the tensile process (in the interval of 1.8%–20.0%) was associated with a large value of $g = 24$, which can be explained by the large number of weak physical cross-links formed by the close intermolecular bonds of the initial molecular structure. These can be bonds formed by pass-through chains between the clusters of the main network of chemical and physical bonds of the elastomer. Clusters—areas of the local structure in amorphous polymers.[13] After the destruction of these intermolecular bonds at the initial stage of tensile deformation, the ascending section of the curve showed a transition to the second main stage of the deformation process (in the range (21%–170%), in which, apparently, a significantly smaller number of pass-through chains between elastomer clusters are involved. In other words, only a fraction of the chemical and physical cross-links were at play here. In this process, the value of M_c was increased and hence the Flory's corrections decreased to $g = 0.6$ (i.e. was less than one).
4. For repeat hysteresis cycles, the process attributed to the initial portion of the ascending strain curve (in the interval of 21%–56%) leg also involves a large number of intermolecular physical cross-links, so $g = 10$. Since clusters may be partially destroyed during the first hysteresis cycle, the tensile process described by the main ascending segments of repeat-cycle curves (in the interval of 65%–164%) are suggested to involve a greater number of the network's chemical cross-links within the clusters. The number of related physical cross-links formed as a result of chain entanglements and chain interlocks will also be greater. Consequently, the value of Flory's correction factor will be greater here than it was in the case of the tensile curve describing the first hysteresis cycle: i.e. $g = 4.5$ (Table 1).

Figure 6 shows the graphs of the dependences based on Eqs. (20) and (21) and the values of Flory's correction factor, g, for the ascending strain curve leg describing the second hysteresis cycle (Fig. 4). Here, the selection of g for the purpose of calculating the rubbery modulus E, using Eq. (21), was made using the maximum value of the correlation coefficient between the linear dependences in Eqs. (20) and (21).

The approximations of Eqs. (20) and (21) for the reverse strain curve legs describing the first and second hysteresis cycles, as well as the related values of g, are shown in Fig. 4. This figure shows the angles of inclination $\frac{b}{k_B T} = -0.0042$ and the degree of straightening $R^2 = 0.9985$ for the main segment (172.5%–103.2%) of the reverse curve of the first hysteresis loop. The value of the Flory correction for this segment $g = 7$.

Table 2 presents the calculated values of g, R^2 and $\pm\frac{b}{k_B T}$ for the experimental reverse deformation curves describing the first (1) and second (2) hysteresis cycles, which are shown in Fig. 4, and are discussed in more detail in Sec. 5 below. The large values of Flory corrections, g for the end segments of these curves, 70 and 81, are 10 times larger than those for the main segments of the decreasing reverse curves. This situation is difficult to explain and requires hypotheses of a strong change in the structure of physical bonds when the rubber is deformed in these areas.

5. The reverse strain curve associated with all of the hysteresis cycles suggest a conclusion to the effect that such reverse curves for rubber feature only two segments. While the crosspiece of the testing machine was moving back to its initial zero-strain position, the stress on the sample decreased exponentially. Calculations based on Eqs. (20) and (21) show that the main process involved in deformation is reversible return deformation of rubber, characterized by a negative slope on Eq. (21), as shown in Fig. 7(a). In the final stage of the reversal curves (65%–25%) an accelerated stress drop occurs, where the slope of the dependence according to Eq. (20), is positive and Flory's correction values are higher, as is evident for each of the final segments 2 in Fig. 7(b). The process behind the first segment of the reverse strain curve describing the first hysteresis cycle (172%–103%) may be explained by the action of the chains coiling back on themselves while carrying along some of the entangled and interlocked structures. These physical cross-links increased Flory's correction factor to $g = 7$. The second segment of the reverse strain curve (65%–25%) takes shape due to the intense intermolecular attraction arising between segments of coiling chains as they approach each other and deformation retardation. This attraction is governed by intermolecular bonds which slow down the movements of the chain fragments, thereby producing a sharp increase in the number of physical cross-links and driving Flory's correction value up to $g = 70$ and $g = 81$ for cycles 1 and 2, respectively.

For comparison, Table 3 shows the values of Flory's correction factor for the entire series of five hysteresis loops obtained at a deformation rate of 250 mm/min at room temperature. Calculated values are listed for the ascending and reverse tensile curves. It is necessary to note five stably repeating segments of the strain curves for the repeated hysteresis loops, in which there is a deceleration or

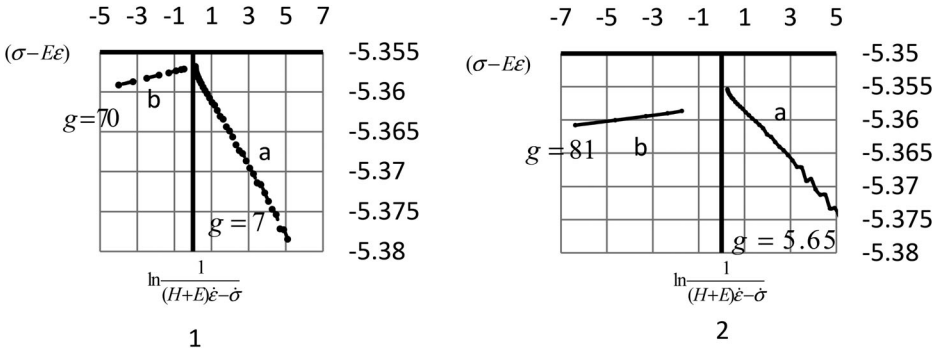

Figure 7. Approximation of Eqs. (20) and (21) for the main segment (a) and the final segment (b) of the reverse strain curve legs describing the first (1) and second (2) hysteresis cycles, as shown in Fig. 4.

acceleration of stress growth or stress drop at a constant strain rate. For an ascending strain curve: segment 1—decelerating of stress growth (Figs. 4 and 5, also Table 1 for the strain intervals 21%–56%); segment 2—accelerating of stress growth (Figs. 4 and 5, also Table 1 for the strain intervals 65%–164%) and segment 3—decelerating of stress growth again (Figs. 4 and 5, also Table 1 for the strain intervals 166%–179%). And for the reverse hysteresis curves: segment 4—decelerating of stress drop (Figs. 4 and 5, also Table 2 for the strain intervals 178%–81%) and segment 5—accelerating of stress drop (Figs. 4 and 5, also Table 2 for the strain intervals 70%–29%).

Table 3 data warrant the following conclusions (5.1–5.8).

5.1. The first hysteresis loop differed significantly from all subsequent loops in the series with identical tensile deformation conditions. Flory's correction for the initial segment of the ascending tensile curve leg was substantially larger than all similar Flory correction values for the initial ascending curve segments in the case of the repeated hysteresis loops.

5.2. For subsequent hysteresis loops, the original closely-packed chain structure was not restored. Residual strain was observed (18.9–25.6% at 25 °C, see Table 8), and the values of Flory's correction factor g go down 2-fold for the initial segment of the ascending strain curve leg. However, they remain quite large and do not change much from one hysteresis cycle to another (ranging between 8.8 and 10 units, Table 3) during the period described by the initial tensile curve segment. Apparently, at the beginning of stretching, the close intermolecular bonds of the initial structure of the coiled chains are broken. This leads to a reduction in the number of chains exerting entropic resistance to the external force. This is reflected in the negative slope for the relationship represented by Eq. (21) (tab. 1 and Fig. 6a) and in reduction of the deformation activation energy.

5.3. For the first hysteresis loop, the main ascending tensile curve segment is based on how some of the shortest inter-junction chains that extend between clusters beginning to stretch and uncoil. As they do so, the clusters gradually begin to disintegrate. The process associated with this curve

Table 8. Residual strain, %, for hysteresis curves obtained at various temperatures and extension rates.

Hysteresis Loop number / Temperature/Extension rate	1	2	3	4	5
25 °C/250 mm/min	18.9	22.14	23.87	25.0	25.6
25 °C/25 mm/min	17.3	20.0	22.0	23.3	24.4
50 °C/25 mm/min	15.4	18.2	20.1	21.4	22.3
75 °C/25 mm/min	14.3	16.7	18.0	18.9	19.4
100 °C/25 mm/min	10.55	12.8	13.9	15.4	16.2

segment does not seem to involve a large number of chemical cross-links or to be accompanied by failures of physical cross-links. This explains why the values of Flory's correction factor for all main ascending tensile curve segments describing only the first hysteresis loop remain significantly below unity. Specifically, g was equal to 0.6 (see Table 3), or 0.1–0.2 for other temperatures (see Tables 5–7 below). Here, the activation energy for the deformation process increased pursuant to Eq. (20). According to Eq. (11), the forces of entropic elasticity generated by the uncoiling chains increase in the direction opposite to that of the increase in strain. Consequently, the activation energy for the ascending strain curve leg increases, as given in Eqs. (12) and (13). This is translated into weak accelerating increase of stress, as observed on tensile curves for elastomers (Figs. 1, 4, and 5).

5.4. For repeat hysteresis loops, the second (main) ascending segment of the strain curve is the region where the entire elastomer network is stretched, and where all intercross linking chains contribute to the growth of the activation energy by creating the forces of entropic elasticity according to Eq. (12). At the same time, the resistance of physical cross-links, having the form entanglements, drives Flory's correction upward. For all repeat hysteresis loops at all measured rates of specimen elongation and temperatures measured, Flory's correction factor stood at *ca.* 5–7 units (see Tables 4–7 below) throughout the length of this ascending curve segment.

5.5. The third (and final) segment of the ascending tensile curve leg reflected a buildup of stress to values so high that the relatively short chains with chemical cross-links would begin to stretch and break. In this scenario, the number of chemical cross-links decreases, as does the number of their physical counterparts. As a result, the values of Flory's correction ($g = 0.1 - 0.3$) become very small, almost 20–100 times smaller than those for the rest of the hysteresis curve segments. This leads to an decrease in the activation energy, E_0, and an decrease in viscosity η due to the decrease in the number of resisting chains, an increase in the value M_c and, accordingly, a decrease in the values g.

5.6. For all hysteresis loops, the main, fourth segment of the inverse deformation curve describes the deformation process, in which all intercross linking chains "help" the crossbar to return to its original position with the zero deformation. These chains coiling and MKU jump into vacancies toward decreasing deformation. This leads to a decrease in the activation energy, E_0, of plastic flow according to Eq. (21) (Fig. 7a). The slope values for

dependence $\frac{1}{\ln(H+E)\dot{\varepsilon}-\dot{\sigma}}$ on $(\sigma - E\varepsilon)$ in Eq. (21) were negative. All entanglements and interlocks (i.e. physical cross-links) contribute to this mass-scale coiling of chemically-linked intercross linking chains. Here, the value of Flory's correction was the same as that for the process described by the main ascending segment of the strain curve (about 5 units). These values were the same for all test extension rates and temperatures.

5.7. For the fifth, the last segment of each reverse curve, Flory's corrections were almost 10–30 times the respective values applied for all the main (second and fourth) segments of the repeat hysteresis curves. This may have to do with the mass-scale formation of close intermolecular bonds by intercross linking chains as they continue coiling. During this coiling process, which occurs at the last stage of deformation, the chains will resist external deformation, which increases the activation energy E_0 and viscosity η of the sample. Here, the tangent $\frac{b}{k_B T}$ of the slope angle for Eq. (20) is positive and Flory's correction values g are in the range from 32 to 150 units (Tables 2–7).

5.8. Overall, the main (second and fourth) segments of the ascending and reverse tensile curves have Flory's corrections of the order of 5–10 units for all temperatures and deformation rates.

Tables 4–7 show the results of hysteresis measurements obtained at a deformation rate of 25 mm/min at room temperature and at 50, 75 and 100 °C, respectively, with the prior results being for a deformation rate of 250 mm/min at room temperature.

As shown by a comparison of Flory's corrections in Tables 3–7 we reached the following conclusions:

1. The numerical values of Flory's corrections were independent of the test temperature and extension rates. We suggest that they reflect the tendency of polymers to preserve a fairly stable structure during mechanical tests.
2. Flory's corrections obtained for repeat hysteresis curves fell close together, so only the first hysteresis curve seems to stand out as different. This is indicative of a change that occurs in the initial polymer structure due to the failure of its weak constituent elements causing the system to move to a more stable and sustainable dynamic elastomer structure. This transition manifests itself in the Mullins effect. As a result of the partial failure of the bonds initially present in the network polymer, the material begins to show a slight residual strain, which changes little during subsequent hysteresis cycles.
3. On the hysteresis curves, five stable segments of the strain curves can be noted. There are three segments for ascending strain and two sections for reverse strain. For each of them, sufficient reproducibility and the characteristic value of the Flory corrections were observed, for all samples.
4. The two main segments of the tensile curves, which are also the longest, *viz.* the second (ascending) and the fourth (reverse), have Flory's correction values which stand close to each other, which means participation of all chains between the chemical cross-links of the elastomer network in these two stages of the deformation process. These structures are almost independent of the number of

hysteresis cycles. Another parameter that seems to remain unchanged is the number of physical cross-links. In the case of the PMVS-based elastomer we have studied, Flory's correction factor,g, had a value of 5–7 units.

5. A high-accuracy description of elastomer deformations can be obtained using the basic equations of the statistical deformation theory and Eyring's formula, modified to account for the entropic nature of deformation in polymers. For the ascending stress segments of the hysteresis curve, these equations indicate an increase in tensile activation energy under the SLS model. For the reverse curve leg, the equations indicate a decrease in deformation activation energy. In this context, the SLS viscosity formula for polymers in a rubber-like state can be written in the following form:

$$\eta = A(\sigma - E\varepsilon)\exp\frac{E_0 \pm b(\sigma - E\varepsilon)}{k_B T} \tag{23}$$

6. The presence of small segments at the start and end of the ascending strain curve leg (identified herein as the first and third segments of the hysteresis cycle) highlight a slowdown in the stress growth process, which can be attributed to a decrease in the process activation energy. At the same time, there was a significant change in Flory's correction values.
7. It is the fifth or end segment of the reverse hysteresis curve that has an especially abrupt (upward) change in the value of Flory's correction factor. This may be interpreted as resulting from a strong growth in the number of physical cross-links due to intermolecular forces arising during the final stage of the elastomer chain-coiling process.

It is, thus, evident that elastomer deformations can be described as a interrelated process. On the one hand, we have the molecular structure as a factor affecting how the deformation will progress, how much and how rapidly the stress will grow and how stiffly the macromolecules will resist the external force when being stretched. On the other hand, we have the strain value as a factor affecting the structural state of the elastomer network formed by the chemical and physical cross-links. This mutual influence pattern is fairly reproducible and consistently recurs in series of measurements of elastomer hysteresis loops.

The principal driver behind this reciprocity is the entropic nature of the forces occurring in macromolecular systems. This peculiarity in deformation behavior of macromolecular solids is ultimately attributable to decreases or increases in the activation energy required for atoms and molecular-kinetic units to migrate into vacant sites during deformation.

Such changes in energy barriers can be viewed as representing increases or decreases in viscosity during the macromolecular stretch-and-flow process. This anomalous feature of macromolecular viscosity affects the deceleration or acceleration of stress growth observed for the different segments of the tensile and reverse-tensile curves when measuring the hysteresis of elastomers.

Conclusions

We have analyzed the relationship between the mechanical properties of elastomers and their network structure. Proceeding from the basic equations of the classic statistical theory of rubber elasticity, we showed that a quantitative evaluation of the effects of labile physical cross-links on the deformation behavior of network elastomers (as determined from rubber hysteresis curves) is actually possible.

The role of physical cross-links in rubber deformations was assessed based on Flory's correction factor, which accounts for how cross-link flaws in network polymers can affect the deformation process flow throughout all stages of extension and recovery in the course of hysteresis.

The use of Eyring's equation (10) viewed through the prism of Frenkel's ideas about the flow mechanism at work in condensed media made it possible to rectify the primary inconsistency found in quantitative descriptions of strain curves for rubbers, *viz.* the discrepancy arising between the theoretical and experimental strain data for elastomers at large strains. This was achieved by modifying the exponential viscous flow equation (10) for polymers by factoring in the decreases or increases in deformation activation energy by amounts that accounts for the entropic elasticity force generated by macromolecules exposed to tensile action.

The Standard Linear Solid (SLS) model was used as a framework for measuring how the stress value depends on the magnitude and rate of strain in calculating the isothermal Young's modulus E. The value of Flory's correction factor g was incorporated in the equations obtained herein (which were linearized as much as possible) as an indicator proportional to the number of physical cross-links arising during deformation and contributing to the deformation behavior.

A study of the repeat hysteresis loops uncovered distinctive, consistently recurring segmentation patterns in the curves describing the deformation behavior of silicone rubbers: the ascending curve legs, were comprised of three segments each, whereas the reverse curve legs were comprised of two segments each.

The calculated data obtained for the experimental hysteresis curves showed good reproducibility of the numerical values of the Flory corrections applied for both tensile and reverse tensile deformations of the sample, as described for each of the identified segments of the curves. The proposed approach makes it possible to easily and quickly determine a value proportional to the number of cross-links present in reticulated elastomeric materials when they are subjected to mechanical stress.

The values of Flory's corrections factors were analyzed with a view to developing hypotheses about how elastomer network structures behave during the individual phases of constant-rate deformation tests (as described by different segments of the respective strain curves, including those comprising the reverse curves of the hysteresis loops).

The findings of this study thus suggest that it is now possible to establish a quantitative correlation between the structural features of network polymers and their mechanical properties.

Acknowledgements

The author expresses his sincere gratitude to Prof. Dr. B. Voigt and Dr. K. Schneider for helping him to conduct the experimental measurements of rubber hysteresis. The author thanks Dr. Yu. Tsoglin for support and discussion of the article.

References

[1] Treloar, L. R. G. *The Physics of Rubber Elasticity*; Clarendon Press: Oxford, UK, **1949**, 254p.
[2] Tobolsky, A. V. *Properties and Structure of Polymers*; John Wiley & Sons, Inc.: New York; London, **1960**, 331p.
[3] Flory, P. J. *Principles of Polymer Chemistry*; Cornell University Press: Ithaca, New York, **1953**, 672p.
[4] Askadskii, A. A. *The Deformation of Polymers*; Khimya: Moskow, **1973**, 448p. (Russian translation).
[5] Diani, J.; Fayolle, B.; Gilormini, P. A Review on the Mullins Effect. *Eur. Polym. J.* **2009**, *45*, 601–612. DOI: 10.1016/j.eurpolymj.2008.11.017.
[6] Golberg, I. I. *Mechanical Behavior of Polymers (the Mathematical Description)*; Khimiya: Moscow, **1970**, 192p. (Russian translation).
[7] Glasstone, S.; Laidler, K. J.; Eyring, H. *The Theory of Rate Processes*; McGraw-Hill: New York, **1941**, 477p.
[8] Frenkel, J. Ueber Die Waermebewegung in Festen Und Fluessigen Koerpern. *Z. Phys.* **1926**, *35*, 652–669. DOI: 10.1007/BF01379812.
[9] Honeycombe, R. W. K. *The Plastic Deformation of Metals*; Edward Arnold: London, **1968**, 408p.
[10] Kartsovnik, V. I.; Worlitsch, R.; Hermann, F.; Tsoglin, Y. Calculation of the Viscosity of Polymer Melts Based on Measurements of the Recovered Rubber-Like Deformation. *J. Macromol. Sci. Part B, Phys.* **2016**, *55*, 149–157. DOI: 10.1080/00222348.2015.1119340.
[11] Kartsovnik, V. I. Changes of Activation Energy during Deformation of Rubber. *J. Macromol. Sci., Part B, Phys.* **2011**, *50*, 75–88. DOI: 10.1080/00222341003641560.
[12] Kartsovnik, V. I. Prediction of the Creep of Elastomers Taking into Account the Forces of Entropic Elasticity of Macromolecules (Prediction of Creep of Elastomers). *J. Macromol. Sci., Part B, Phys.* **2018**, *57*, 447–464. DOI: 10.1080/00222348.2018.1470386.
[13] Boyer, R. F. Evidence from T*ll* and Related Phenomena for Local Structure in the Amorphous State of Polymers. In *Order in the Amorphous "State" of Polymers*; Steven E. Keinath, Robert L. Miller, and James K. Rieke, Eds.; Plenum Press: New York and London, **1987**.